

Attenuation of Millimeter Emission from Circumstellar Disks Induced by the Rapid Dust Accretion¹

Taku Takeuchi^{1,2} and D.N.C. Lin²

ABSTRACT

From millimeter observations of classical T Tauri stars, it is suggested that dust grains in circumstellar disks have grown to millimeter size or larger. However, gas drag on such large grains induces rapid accretion of the dust. We examine the evolution of dust disks composed of millimeter sized grains, and show that rapid accretion of the dust disk causes attenuation of millimeter continuum emission. If a dust disk is composed mainly of grains of $1\text{ cm} \sim 1\text{ m}$, its millimeter emission goes off within 10^6 yr. Hence, grains in this size range cannot be a main population of the dust. Considering our results together with grain growth suggested by the millimeter continuum observations, we expect that the millimeter continuum emission of disks comes mainly from grains in a narrow size range of $[1\text{ mm} \sim 1\text{ cm}]$. This suggests either that growth of millimeter sized grains to centimeter size takes more than 10^6 yr, or that millimeter sized grains are continuously replenished. In the former case, planet formation is probably difficult, especially in the outer disks. In the latter case, reservoirs of millimeter grains are possibly large ($\sim 10\text{ m}$) bodies, which can reside in the disk more than 10^6 yr. Constraints on the grain growth time-scale are discussed for the above two cases.

Subject headings: accretion, accretion disks | planetary systems: formation | solar system: formation

1. Introduction

Observations at millimeter wavelengths ($\sim 1 \sim 3\text{ mm}$) have revealed that about 50% of classical T Tauri stars (CTTSs) emit detectable millimeter continuum. The detection limit, $10 \sim 20\text{ mJy}$, of the 1.3 mm observations by Osterloh & Beckwith (1995) corresponds to a minimum disk luminosity of $4 D^2 F_{1.3} \sim 5 \times 10^8\text{ erg s}^{-1}$, where we used the distance to the Taurus-Auriga molecular cloud, $D = 140\text{ pc}$, while the typical value of the disk luminosity is $10^{29} \sim 10^{31}\text{ erg s}^{-1}$ (Beckwith et al. 1990; Ohashi et al. 1991, 1996). The sizes of the disks that emit millimeter continuum are in a range between $100 \sim 500\text{ AU}$ (Dutrey et al. 1996; Kitamura et al. 2002). Only a small fraction ($\sim 10\%$) of weak line T Tauri

stars (WTTs), however, have detectable emission at 1.3 and 2.7 mm (Osterloh & Beckwith 1995; Dutrey et al. 1996; Duvert et al. 2000). It is not clear whether the typical age of WTTs is older than that of CTTSs, as both classes have similar age distributions between 10^5 and 10^7 yr (Kenyon & Hartmann 1995). However, the observations have made clear that the outer part ($\sim 100\text{ AU}$) of the disk that emits millimeter continuum disappears in a timescale between 10^6 and 10^7 yr. The standard interpretation assumes that WTTs are the older counterparts of CTTSs.

A notable feature of the millimeter emission from CTTSs is the evolution of the spectral index from the interstellar value. The frequency dependence of the dust emissivity (or the opacity) is conventionally expressed as a power law, $\kappa_\nu \propto \nu^\beta$, where ν is the frequency of radio emission. Beckwith & Sargent (1991) argued that the value of the opacity index evolves from the interstellar value of 2 to ~ 1 for CTTS disks (see also Mannings & Emerson 1994; Hogerheijde et al. 2003).

¹Earth and Planetary Sciences, Kobe University, Kobe 657-8501, Japan; taku@kobe-u.ac.jp

²UCO/Lick Observatory, University of California, Santa Cruz, CA 95064; lin@ucolick.org

¹Accepted by ApJ

This change in τ is probably due to dust evolution in the disks. However, because different directions of dust evolution (such as in grain size, in chemical composition, and in grain shape) can produce observable changes in the dust opacity, it is not easy to specify the cause of changing τ (Beckwith, Henning, & Nakagawa 2000). Among the above possible causes, dust growth is an attractive hypothesis in a context of planet formation. The effect of dust growth on the dust opacity was studied by Miyake & Nakagawa (1993). Their calculations showed that grain growth to 1 mm would produce a low τ value (~ 1), but that it is difficult to explain $\tau \sim 1$ as long as the maximum size of grains is smaller than 1 mm. In this paper, we stand at the ground that the low τ is a sign of dust growth, and we assume that in the disks showing $\tau \sim 1$ the dust grains have grown to ~ 1 mm.

In summary, radio observations have shown that about half of CTTSs emit detectable millimeter continuum. In ages of millimeter continuum show extended disks of 100–500 AU in size, while their wavelength dependences show the evolution of τ , suggesting grain growth to ~ 1 mm. Millimeter continuum emissions of CTTSs last for 10^6 – 10^7 yr.

Dust grains in a gas disk migrate to the central star due to gas drag (see §2.2). As grains grow larger, their orbital decay time becomes shorter. When the grain size becomes 1 cm, the decay time is only about 10^5 yr, which is much shorter than the dust disk's lifetime observed for CTTSs. This dust growth and subsequent dust accretion induce a decline in millimeter emission from the disk. The millimeter emission would disappear in 10^5 yr, if most of the dust mass had been condensed in the largest grains of ~ 1 cm. Thus, we expect that in CTTS disks, there must remain sufficient dust grains less than 1 cm over 10^6 yr. This expectation is confirmed in §4 using numerical calculations. At the same time, however, the largest grain size must be larger than about 1 mm, if low τ is due to dust growth. Very large bodies (say ~ 10 m) experience little migration, because such bodies almost completely decouple from the gas. However, such large bodies do not contribute to millimeter emission (Miyake & Nakagawa 1993). Hence, in this paper we conclude that only a narrow range of the dust size, [1 mm; 1 cm], can fulfill the requirement that the millimeter continuum having $\tau \sim 1$

lasts over 10^6 yr.

Our calculations suggest that the millimeter continuum of CTTS disks is mainly emitted from grains of 1 mm–1 cm. Thus, the lifetime of observable millimeter continuum, 10^6 – 10^7 yr, constrains the growth time of millimeter-sized grains. One possibility is that millimeter-sized grains do not grow to centimeter size in 10^6 yr and they hold the millimeter continuum of $\tau \sim 1$. Another possibility is rapid growth of grains in a context of planet formation: grains in CTTS disks have already grown to sizes of ~ 10 m, which is large enough to resist gas drag and to reside in the disk more than 10^6 yr. We consider these possibilities in §5.

2. Dust Properties in Disks

2.1. Assumption of the Largest Size of Grains

The observations discussed in the last section suggest that dust grains in circumstellar disks have grown to at least 1 mm. It is possible to consider that even at the CTTS stage of 10^6 yr the dust grains have grown to sizes much larger than 1 mm. However, the observations have not set any constraint on the largest size, and thus we know only its lower limit, ~ 1 mm. In order to choose a specific question, we focus on the epoch at which the largest grains have just grown to 1 mm, i.e., we assume that the largest size is of order of 1 mm. At such an epoch, the dust mass and the opacity are dominated by the largest grains (~ 1 mm) as discussed below. Hence, in the later sections, we consider only a single size of the largest grains.

2.2. Dust Radial Migration

Dust grains migrate inward to the star under the action of gas drag. The gas experiences a pressure gradient force, which usually cancels a part of the central star's gravity and induces slower rotation than the Keplerian velocity. Dust grains, whose orbits are hardly affected by gas pressure, are supposed to rotate with Keplerian velocity, but experiencing headwind. They lose their angular momentum and spiral inward to the central star (Adachi, Hayashi, & Nakazawa 1976; Weiden-schilling 1977).

In this paper, we mainly consider dust grains

smaller than 1 cm. For such small grains, gas drag obeys Epstein's law, which is applicable when the mean free path of the gas molecules is larger than the grain size (The mean free path is 7 cm at 1 AU and larger at larger radii in our standard model; see e.g., Nakagawa, Sekiya, & Hayashi 1986). The gas drag force on a spherical grain is given by

$$F_g = \frac{4}{3} \rho_g s^2 v_t (v_d - v_g); \quad (1)$$

where ρ_g is the gas density, s is the grain radius, $v_t = (8\pi)^{1/2} c$ is the mean thermal velocity of gas molecules, c is the gas sound speed, and v_d and v_g are the velocities of the grain and the gas, respectively. The stopping time due to gas drag is $t_s = m_d (v_d - v_g) / F_g$ where $m_d = \frac{4}{3} \rho_p s^3$ is the grain mass, and ρ_p is the physical density of an individual grain. We define the non-dimensional stopping time normalized by the orbital time as,

$$T_s = t_s \Omega_K = \frac{\rho_p s v_K}{\rho_g r v_t}; \quad (2)$$

where r is the distance from the star, $\Omega_K = (GM/r^3)^{1/2}$ is the Keplerian angular velocity, $v_K = r \Omega_K$ is the Keplerian velocity, and M is the central star's mass.

The stopping time is proportional to the grain size, which means that the gas drag force is more effective for smaller grains. If a grain is small enough to have a stopping time much less than its orbital time ($T_s \ll 1$; this is true for grains of $s \lesssim 1$ cm), it orbits with the almost same angular velocity as the gas has, which is sub-Keplerian (Adachi et al. 1976; Weidenschilling 1977). Therefore, the centrifugal force on the grain is smaller than the stellar gravity, resulting in an inward acceleration by the residual gravity. This acceleration is however balanced by gas drag in the radial direction. After a stopping time-scale, which is smaller than the orbital time, the grain reaches a terminal falling velocity. This terminal velocity is slower for smaller grains because the stronger gas drag force per unit mass holds the grains more tightly with the gas. For large grains of $T_s > 1$, the coupling between the grains and the gas is weak. They rotate with Keplerian velocity and experience headwind from the gas. The inward drift speed of the grains is proportional to the angular momentum loss by gas drag ($\propto s^2$) per unit mass ($\propto s^2/s^3$). Thus, larger grains drift more slowly

for $T_s > 1$ regime. Figure 1 shows the orbital decay time (or the migration time τ_{dust} defined in x3.4) of grains at 50 AU in a disk model described below in x3.1. (Epstein's law is valid for $s \lesssim 1$ km at 50 AU. We used eq. [15] described below to calculate $\tau_{\text{dust}} = r/v_d$ assuming the gas accretion velocity $v_g = 0$.) For compact grains (the particle physical density $\rho_p = 1$ g cm⁻³; solid line), the orbital decay time of [100 μ m – 10 m] grains is less than 10⁶ yr, and it has a minimum value of 5×10^3 yr when the size is 5 cm. For fluffy grains ($\rho_p = 0.1$ g cm⁻³; dashed line), the plot of orbital decay time in Figure 1 shifts rightward with a 10 fold increase in the grain size. From this figure, it is expected that grains of $\rho_p = 0.1$ – 1 g cm⁻³ in the size range [1 mm – 10 m] disappear from the disk within 10⁶ yr because of rapid accretion to the central star.

2.3. Dust Opacity

We focus on the optical property of the dust at millimeter wavelengths, $\lambda \sim 1$ mm. As we assumed that the maximum size is of order of 1 mm, most grains are similar to or smaller than the observation wavelength, $\lambda \sim 1$ mm. The optical properties of such grains can be described according to Rayleigh scattering theory. The absorption cross section, σ_{abs} , of a spherical grain is proportional to its volume or mass (van de Hulst 1981), i.e.,

$$\sigma_{\text{abs}} = \frac{4 \pi m^0}{\rho} m_d; \quad (3)$$

where m^0 is the imaginary part of the refractive index, λ is the wavelength, and $m_d = \frac{4}{3} s^3 \rho_p$ is the grain mass. The cross section per unit mass is independent of the grain size: $\sigma_{\text{abs}}/m_d = 4 \pi m^0 / (\rho_p \lambda)$.

Suppose a power-law grain size distribution. The number density of grains in a unit size range is

$$n(s) = n_0 \frac{2}{s} : \quad (4)$$

The total cross section of grains in a unit volume is

$$\begin{aligned} \sigma_{\text{tot}} &= \int_{s_{\text{min}}}^{s_{\text{max}}} \sigma_{\text{abs}} n(s) ds \\ &= \frac{8}{3(4\pi)} \frac{2}{\lambda} n_0 m^0 (s_{\text{max}}^4 - s_{\text{min}}^4) \end{aligned} \quad (5)$$

where s_{\min} and s_{\max} are the minimum and maximum sizes of grains. If β is less than 4, the cross section is dominated by the largest grains. In such a case, it is adequate to take only the largest grains in consideration of the dust opacity.

When the largest grains have grown to sizes larger than $10 \mu\text{m}$, it is expected that the dust size distribution of the disk has a void between $[1 \text{ mm} - 10 \mu\text{m}]$, because of rapid accretion of grains to the star in this size range, as discussed in §2.2. In addition, grains larger than $10 \mu\text{m}$ hardly contribute to millimeter emission. The mass opacity of $10 \mu\text{m}$ grains is 10^{-3} times smaller than 1 mm grains (Fig. 4 in Miyake & Nakagawa 1993). If most of the dust mass is concentrated in bodies larger than $10 \mu\text{m}$, the dust cannot emit a millimeter flux strong enough to explain the observed values of CTTs. Hence, in consideration of the millimeter emission, the contribution of bodies larger than $10 \mu\text{m}$ can be neglected.

2.4. Dust Growth

The size distribution of grains in the interstellar medium is considered to be a power-law with $\beta = 3.5$ (Mathis, Rumpl, & Nordsieck 1977). In circumstellar disks, however, the grains stick together and grow larger. The size distribution probably changes through this process. Mizuno, Markiewicz, & Volk (1988) found from their numerical simulations that after the grain growth more mass concentrates in the largest grains and that the power-law index becomes as small as $\beta = 1.9$. On the other hand, collisional destruction of grains may lead to a different distribution. Hellyer (1970) analytically derived a power-law index $\beta = 3.5$ for particles experiencing collisional fragmentation. While this is in agreement with the observed distribution of asteroids of sizes between $30 - 300 \text{ km}$, recent observations show a shallower index for small asteroids of $< 5 \text{ km}$ (Yoshida et al. 2003). In either case, the largest bodies dominate the dust mass and the dust opacity at 1 mm , as long as the largest size is less than 1 mm .

In conclusion, the above considerations in §2.3 and §2.4 suggest focusing on the largest grains of 1 mm .

In the following sections, we investigate evolution of the dust density profile and the thermal flux emitted at millimeter wavelengths, both of which are dominated by the largest grains.

3. Model Equations and Assumptions

As discussed in the last section, we consider disks at the epoch in which the largest grains are of order of 1 mm , and focus on the largest grains. We solve for the density evolution of a dust disk, assuming all grains are of a similar size of 1 mm . Contributions from smaller grains are neglected. In the numerical calculations, the grain size is assumed to be constant with time and any effect caused by dust growth is ignored. From the numerical results, however, we discuss the constraint on the dust growth time-scale in §5 below.

3.1. Model Assumptions and the Initial Disk

For simplicity, we assume that the gas disk has a power-law temperature profile T in the radial direction r , and is isothermal in the vertical direction z . The profile is written as

$$T(r) = T_0 r_{\text{AU}}^q; \quad (6)$$

where the subscript "0" denotes quantities at 1 AU , and a non-dimensional quantity r_{AU} is the radius in AU . We assume that the temperature profile does not change through the disk evolution. The initial surface density distribution Σ_g is also a power-law,

$$\Sigma_g(r; t=0) = \Sigma_{g,0} r_{\text{AU}}^p; \quad (7)$$

and is truncated at $r_{\text{out}} = 100 \text{ AU}$. The isothermal sound speed is $c = c_0 r_{\text{AU}}^{q/2}$ and the gas disk scale height h_g is thus defined as ⁴

$$h_g(r) = \frac{c}{K} = h_0 r_{\text{AU}}^{(q+3)/2}; \quad (8)$$

The disk has a turbulent viscosity η_t . In this paper, we simply model the viscous effect of turbulence using the so-called α -prescription (Shakura & Sunyaev 1973),

$$\eta_t = \alpha h_g = \alpha_0 h_0 r_{\text{AU}}^{q+(3/2)}; \quad (9)$$

Most of the dust mass is concentrated in the largest grains. Therefore, we assume all grains

⁴Strictly speaking, the scale height of an isothermal disk is $\sqrt{2}h_g$, because the gas density varies as $\rho_g / \exp[-z^2/(2h_g^2)]$.

have the same size, which is of order of 1 mm. Initially, the dust spreads over the entire gas disk, and its density profile ρ_d is proportional to the gas density:

$$\rho_d(r; t=0) = f_{\text{dust}} \rho_g = f_{\text{d},0} r_{\text{AU}}^p; \quad (10)$$

where the initial dust-to-gas ratio f_{dust} is independent of r . Most of the disk is outside the ice condensation radius (~ 3 AU), and the main composition of the dust is water ice. We ignore sublimation of water ice at the innermost part of the disk, because our interest is on the outer part that contributes to millimeter emission. The physical density of a compact grain is assumed to be $\rho_p = 1 \text{ g cm}^{-3}$. If grains are fluffy (porous) and include vacuum inside their volume, the density is smaller.

We adopt the following fiducial parameters: $M = 1 M_\odot$, $\rho_{g,0} = 3.5 \times 10^2 \text{ g cm}^{-2}$, $h_0 = 3.33 \times 10^2 \text{ AU}$, $p = 1$, $q = \frac{1}{2}$, $r_{\text{out}} = 100 \text{ AU}$, and $\beta = 10^{-3}$. These values correspond to a disk having a gas mass of $M_g = 2.5 \times 10^2 M_\oplus$ inside 100 AU (the mass within 40 AU is $10^2 M_\oplus$, which is comparable to the minimum-mass-solar-nebula model of the standard theory of planet formation; Hayashi, Nakazawa, & Nakagawa 1985). The temperature distribution is $T = 278 r_{\text{AU}}^{1/2} \text{ K}$ (Hayashi et al. 1985). Radio observation by Kitamura et al. (2002) suggests that the power law index of the surface density profile, p , is between $-1.5 < p < 0$. For dust grains, we use $f_{\text{dust}} = 10^{-2}$, $s = 1 \text{ mm}$, and $\rho_p = 1 \text{ g cm}^{-3}$.

3.2. Equations for the Density Evolution

Evolution of a gas disk occurs due to viscous torque (Lynden-Bell & Pringle 1974). The torque exerted on the disk gas outside r by the inner disk is $2\pi r^2 \rho_g r^3 d\Omega_K = dr$. The differential between the torques exerted from the inside and from the outside causes a radial motion of the gas. Assuming that the gas rotation velocity is always Keplerian, the gas radial velocity becomes

$$v_g = \frac{3}{r^{1/2}} \frac{d}{g} \frac{dr}{dt} (r^{1/2} \rho_g); \quad (11)$$

as derived in equation (12) of Lin & Papalizou (1986; with no planetary torque). The gas density ρ_g obeys the equation of continuity,

$$\frac{\partial}{\partial t} \rho_g + \frac{3}{r} \frac{\partial}{\partial r} (r^{1/2} \frac{\partial}{\partial r} (r^{1/2} \rho_g)) = 0; \quad (12)$$

The equation of continuity for the dust density ρ_d is

$$\frac{\partial}{\partial t} \rho_d + \frac{1}{r} \frac{\partial}{\partial r} [r(F_{\text{dif}} + \rho_d v_d)] = -\dot{\rho}_d; \quad (13)$$

where F_{dif} is the diffusive mass flux, v_d is the dust radial velocity, and $-\dot{\rho}_d$ is the mass loss rate of the dust due to grain growth. The mass flux comes from two terms. One is the mass flux caused by diffusion of grains in the turbulent gas. The diffusion works to smooth out any fluctuation in the dust concentration $\rho_d = \rho_g$. We adopt the assumption that the diffusive mass flux is proportional to the concentration gradient, and that the diffusion coefficient is the same as the gas viscosity. This assumption is applicable to small passive grains tightly coupled to the gas ($T_s \gg 1$ and the Schmidt number $Sc = 1$). The diffusive mass flux F_{dif} is defined by

$$F_{\text{dif}} = -\pi r^2 \rho_g \frac{\partial}{\partial r} \left(\frac{\rho_d}{\rho_g} \right); \quad (14)$$

The other contribution to the mass flux is from the dust radial motion induced by gas drag and is written as $\rho_d v_d$. The dust radial velocity, v_d , caused by gas drag is calculated in equation (23) of Takeuchi & Lin (2002; henceforth Paper I) as

$$v_d = \frac{T_s^{-1} v_g}{T_s + T_s^{-1}} \chi_K; \quad (15)$$

where χ_K is a factor relating the gas rotation velocity to its Keplerian value. The gas disk has a radial pressure gradient, $\partial P_g / \partial r$, which cancels a part of the stellar gravity and leads to a slower gas rotation than the Keplerian velocity. We define χ_K as the ratio of the pressure gradient to the gravity,

$$\chi_K = \frac{1}{r^2} \frac{\partial P_g}{\partial r}; \quad (16)$$

Because the gravity is reduced by a factor $(1 - \chi_K)$, the angular velocity of the gas becomes

$$\Omega_g(r) = (1 - \chi_K) \Omega_K(r); \quad (17)$$

As discussed in Paper I, the gas rotation velocity and χ_K are functions of the height z from the midplane. The stopping time T_s also varies because the gas density changes with z . In the calculation of the dust velocity in equation (15), we

use the midplane values for ρ_g and T_g . This is because grains as large as 1 mm sediment to the midplane and most grains are concentrated at the midplane. (Concentration of 1 mm grains is not strong enough to induce a change in the gas velocity profile at the midplane, provided that $\beta \ll 10^{-4}$. The midplane dust density does not exceed the gas density, as discussed in §5.3 below. We use the gas radial velocity of eq. [11], which is the averaged value over the z-direction. The outward motion of the midplane gas proposed by Paper I is neglected, because it has a significant effect only at the innermost part ($r \lesssim 3$ AU) in which the first term of eq. [15] dominates the dust velocity.) At the midplane, the gas density is (eq. [6] of Paper I)

$$\rho_g = \frac{p_g}{2 h_g} : \quad (18)$$

The pressure is calculated from the isothermal equation of state as

$$p_g = c^2 \rho_g = \frac{h_g^2}{2} \rho_g : \quad (19)$$

Using the power-law expression of the disk scale height (8) and the Kepler rotation law $\Omega_K \propto r^{-3/2}$, we have the midplane value

$$= \frac{h_g^2}{r} \frac{d \ln \rho_g}{d \ln r} + \frac{q}{2} : \quad (20)$$

Similarly, using equations (2), (8) and $v_t = \beta c$, the non-dimensional stopping time at the midplane is

$$T_s = \frac{p_g}{2 \rho_g} : \quad (21)$$

In the right-hand-side in equation (13), a sink term $-\dot{m}_d$ is added to represent a mass loss of the dust. The mass loss is caused by grain growth and subsequent rapid accretion to the star. Detailed definition of the mass loss is discussed in §5 below.

3.3. A Convenient Non-dimensional Parameter

In a gas disk with given profiles of ρ_g and Ω , the dust density evolution is controlled only via the stopping time T_s (see eqs. [13] and [15]). If different sets of the dust parameters $f s; p_g$ have the same stopping time, evolutions of these dust disks are the same (we assume the sink term $-\dot{m}_d = 0$). In

addition, scaling the gas density does not change the gas evolution (see eq. [12]). That is, if the initial gas mass (or $\rho_{g,0}$ in eq. [7]) is altered without changing the shape of the density profile (p in eq. [7]), we have the same gas evolution except for the scaling factor. Throughout this paper, we consider only the case of $\rho_g \propto r^{-1}$ and $r_{\text{out}} = 100$ AU. The dust evolution depends also on the initial gas mass through the stopping time (eq. [21]). However, we can retain the same dust evolution for different values of the initial gas mass by adjusting the dust parameters to keep the same stopping time. For parameter sets of the gas mass M_g within 100 AU, the grain size s , and the particle physical density p , if we have the same value of

$$A = \frac{M_g}{2.5 \times 10^2 M} \frac{s}{1 \text{ mm}} \frac{p}{1 \text{ g cm}^{-3}} ; \quad (22)$$

then we have the same stopping time and the same dust evolution. (If the initial profile of the gas surface density is different from $\rho_g \propto r^{-1}$, we have different dust evolution even for the same value of A .)

For example, the parameter sets $f M_g; s; p_g = f 2.5 \times 10^2 M; 1 \text{ mm}; 1 \text{ g cm}^{-3} g$, $f 2.5 \times 10^2 M; 10 \text{ mm}; 0.1 \text{ g cm}^{-3} g$, and $f 2.5 \times 10^1 M; 10 \text{ mm}; 1 \text{ g cm}^{-3} g$ have the same $A = 1$. We call these parameter sets "A = 1 model". The other parameter sets considered in this paper have $A = 0.1$ or 10. The parameter sets of $A = 0.1$ model are, for example, $f M_g; s; p_g = f 2.5 \times 10^1 M; 1 \text{ mm}; 1 \text{ g cm}^{-3} g$ or $f 2.5 \times 10^2 M; 1 \text{ mm}; 0.1 \text{ g cm}^{-3} g$. In A = 10 model, we have for example $f M_g; s; p_g = f 2.5 \times 10^3 M; 1 \text{ mm}; 1 \text{ g cm}^{-3} g$ or $f 2.5 \times 10^2 M; 10 \text{ mm}; 1 \text{ g cm}^{-3} g$.

We note that the millimeter continuum flux from the dust disk depends on the disk mass (nearly proportional to the total dust mass). When calculating millimeter flux, we specify the gas disk mass M_g , in addition to the value of A . If the dust sink term $-\dot{m}_d$ is considered, the disk evolution varies independently with s , p , and M_g .

Figure 2 shows the non-dimensional stopping time for various values of A . The non-dimensional stopping time is less than unity in most cases of our models. Grains are tightly coupled to the gas except at the outermost part of the disk of $A = 10$.

3.4. Accretion Time Scale of the Gas and the Dust

The gas accretion time-scale τ_{gas} is of order of the viscous time-scale $\tau^2 = \tau$. Here, we define it as $\tau_{\text{gas}} = r/v_g$, where the gas radial velocity is given by equation (11). From equation (9), the viscosity η is proportional to r in the models with $q = \frac{1}{2}$, and then the accretion time τ_{gas} is also proportional to r , as shown by the dashed line in Figure 3. The accretion time is of order of 10^7 yr at 100 AU when the viscosity parameter is $\alpha = 10^{-3}$. This means that disks with an initial radius of 100 AU keep their gas for 10^7 yr.

The inward migration time of the dust is defined by $\tau_{\text{dust}} = r/v_d$, where the dust radial velocity written in equation (15) is induced by gas drag. The stopping time due to gas drag is smaller than the orbital time in most cases considered here, i.e., $T_s < 1$, and grains are tightly coupled to the gas, as shown in Figure 2. From equations (15) and (21), the radial velocity of small grains that have $T_s \ll 1$ becomes

$$v_d = v_g - \frac{\rho_p S V_K}{2 \rho_g}; \quad (23)$$

which means that the radial drift velocity from the gas (the second term) is proportional to the grain size and the particle physical density, and is inversely proportional to the gas density.

Figure 3 shows the dust migration time τ_{dust} for various models. Model of $A = 1$ represents, for example, 1 mm grains with $\rho_p = 1 \text{ g cm}^{-3}$ in a disk of a mass $M_g = 2.5 \times 10^2 M_J$ inside 100 AU. In this case, the migration time is about 10^5 yr and does not vary significantly with r . The time-scale is much shorter than the gas accretion time-scale in most part of the disk. Hence, we expect such grains are quickly accreted onto the star and removed from the disk. The migration time is even smaller for larger grains or for a smaller gas mass in $A = 10$ model. Outside 200 AU, the migration time increases with r , because the non-dimensional stopping time is larger than unity at such a region (see Fig. 2), and the dust velocity decreases with decreasing ρ_g (see eqs. [15] and [21]). In $A = 0.1$ model, i.e., if grains are μm ($\rho_p = 0.1 \text{ g cm}^{-3}$) or if the gas disk is massive ($M_g = 2.5 \times 10^1 M_J$), then the dust migration time can be as long as 10^6 yr in the outer part of the disk ($r \sim 50 \text{ AU}$).

4. Evolution of the Dust Distribution

We first show how the radial motion of the dust accelerates evolution of the dust density and of its millimeter emission. In this section, the sink term due to grain growth in equation (13) is set to zero, i.e., $\dot{\rho}_d = 0$. The effect of grain growth is considered in §5 below.

4.1. Numerical Method

We solve equations (12) and (13) numerically in order to obtain evolution of the density profiles of the gas and the dust.

Equation (12) for the gas is a diffusion equation. We solve the equation using the standard implicit method, the Crank-Nicholson scheme (Press et al. 1992). The numerical mesh is uniformly spaced in a logarithmic space of $[r_1; r_2] = [1; 10^3] \text{ AU}$ by 200 grid points. For boundary conditions, we simply assume that the density at the inner and outer boundaries are zero, i.e., $\rho_g(r_1) = \rho_g(r_2) = 0$ (Bath & Pringle, 1981; Amatei et al. 2003).

For the dust, equation (13) is composed of the terms of diffusion, $\partial(rF_{\text{dif}})/\partial r$, and of advection, $\partial(r v_d \rho_d)/\partial r$. Each contribution of these terms to the time evolution is numerically solved in separate steps. The diffusion part is solved with the Crank-Nicholson scheme. The advection part is solved with the monotonic second order scheme (van Leer 1977). We use the same boundary conditions as the gas, i.e., $\rho_d(r_1) = \rho_d(r_2) = 0$.

The inner boundary condition, $\rho_g(r_1) = 0$, induces an artificial positive density gradient on the close neighborhood of the boundary. We regard that the evolution of the main body of the gas disk will not be affected seriously by this boundary condition. For the dust, however, the positive gas density gradient leads to a positive gas pressure gradient and thus $\dot{\rho}_d < 0$, which raises an artificial outward motion of the dust (see eqs. [15] and [16]). To suppress this outward motion, we simply set $\dot{\rho}_d = (\rho_g/r)^2 (q - 3)/2 (> 0)$, neglecting the term $d(\ln \rho_g) = d(\ln r)$ in equation (20), in the inner-edge zone where the gas density gradient is positive.

4.2. Low Viscosity Models

First, we discuss disks with a low viscosity. When the viscosity parameter is $\alpha = 10^{-3}$, the

gas accretion time-scale at the outer disk radius (100 AU) is 10^7 yr. The gas disk survives viscous draining for 10^7 yr. Grains of $s = 1$ mm and $\rho_p = 1$ g cm $^{-3}$, however, have migration time as small as 10^5 yr, and accrete much more quickly to the star.

Figure 4a shows the surface density evolution of the gas and the dust in $A = 1$ model. While the outermost part of the gas disk expands, the inner part accretes inward. The gas surface density in a region $[1; 100]$ AU slowly decreases from the initial value. Although the dust disk has the same initial density profile as the gas except for the dust-to-gas ratio f_{dust} , it experiences quite a different evolution. The inward drift velocity is large, and none of the dust can expand beyond the initial outer radius of 100 AU. The entire dust disk rapidly accretes to the star. In 10^6 yr, most of the dust has fallen to the star. A dust disk of $A = 1$ can not survive for 10^6 yr.

The expression of the dust radial velocity (23) shows that the dust has a slower velocity if the particle physical density is smaller or if the gas density is higher. In such cases, the gas drag force is more effective at keeping the grains tightly entrained to the slow, gas accretion motion. The dust density evolution of $A = 0.1$ model is 10 times slower than $A = 1$ model, as shown in Figure 4b. The dust disk can survive over 10^6 yr in this case.

When the grains grow larger, however, the dust returns to a faster migration velocity, as shown in equation (23). Even in the cases where the dust is μm ($\rho = 0.1$ g cm $^{-3}$) or the gas disk is massive ($M_g = 0.25 M_\odot$), if the grain radius is 1 cm, then we have again $A = 1$ and the dust accretes rapidly in 10^5 yr. The dust density evolution goes back to $A = 1$ model shown in Figure 4a.

Evolution of the dust density causes attenuation of thermal emission from the disk. The thermal flux F observed at a frequency ν is (Adams, Lada, & Shu 1988)

$$4 D^2 F_\nu = 4 \int_{r_{\text{in}}}^{r_{\text{out}}} B_\nu(T) [1 - \exp(-\tau_\nu)] 2\pi r dr; \quad (24)$$

where D is the distance of the disk from the observer, B_ν is the Planck function, τ_ν is the vertical optical depth of the disk. For simplicity, we assumed that the disk is observed face-on from a distance of $D = 140$ pc. Because most of the millimeter

flux comes from the optically thin, outer part of the disk, the viewing angle does not affect the flux significantly, unless the disk is close to edge-on. The optical depth is $\tau_\nu = \kappa_\nu f_{\text{dust}}$, where the opacity κ_ν is defined for unit mass of the initial disk gas that is well mixed to the dust (with the dust-to-gas ratio $f_{\text{dust}} = 0.01$), and thus $\kappa_\nu = f_{\text{dust}} \kappa_{\nu, \text{dust}}$ is the opacity for unit dust mass. We assume that the dust opacity index is $\beta = 1$ and $\kappa_{\nu, \text{dust}} = 0.1$ ($= 10^{12}$ Hz), which is observationally suggested (Beckwith & Sargent 1991; Kitamura et al. 2002). The millimeter flux is nearly proportional to the disk mass. We assume an initial disk mass $M_g = 2.5 \times 10^{-2} M_\odot$. Figure 5 shows the time evolution of the disk emission at 1.3 mm wavelength, compared to observations by Beckwith et al. (1990) and Osterloh & Beckwith (1995). In $A = 1$ model, the disk emission quickly decays and in 6×10^5 yr it becomes lower than the detection limit. To keep the thermal emission over 10^6 yr, the dust grains must be μm or the gas disk must be massive, as shown by the result for $A = 0.1$ model. (In cases of massive disks, the magnitude of the millimeter flux would be larger than the line of $A = 0.1$ in Fig. 5, which is drawn for $M_g = 2.5 \times 10^{-2} M_\odot$.) Even in the μm dust or massive disk cases, however, grain growth from 1 mm to 1 cm recovers $A = 1$, and then the emission decays in 6×10^5 yr.

4.3. High Viscosity Models

Figure 6 shows the dust density evolution of a disk with a viscosity parameter $\alpha = 10^{-2}$. The gas disk suffers rapid viscous accretion and in 10^6 yr the gas density within 100 AU reduces significantly.

On the other hand, because the dust drift velocity (the second term in eq. [23]) is independent of α , evolution of the dust disk does not differ significantly from the models with low viscosity ($\alpha = 10^{-3}$), except that the dust accretion is slightly faster. In $A = 0.1$ model shown in Figure 6b, the dust migration time-scale at the initial state ($t = 0$) is comparable to the gas lifetime of 10^6 yr. As the gas density declines, however, the dust accretion is sped up (see eq. [23]). We have thus a faster dust accretion than in the low viscosity case. The dust always disappears before the gas dispersal. Evolution of the millimeter emission shown in Figure 7 is similar to the low viscosity

models, but is a few times faster.

4.4. Meter Sized Bodies

We consider a case in which the largest bodies have grown to meter size. The non-dimensional stopping time of meter sized bodies is larger than unity and the drift velocity is smaller for larger bodies as shown in Figure 1. Thus, there is a lower limit for the body size to survive in a disk for 10^6 yr. Figure 8 shows the evolution of the dust disks for 1 m and 10 m bodies. The gas mean free path is less than 1 m in the inner disk of $r \leq 4$ AU, and less than 10 m for $r \leq 10$ AU. Epstein's drag law is thus not valid in the innermost part of the disk, but we neglect the divergence from the Epstein's law because our interest is mainly on the outer part. For bodies of $T_s \ll 1$, the gas drag does not cause any significant diffusion of the dust, so we set $F_{\text{diff}} = 0$ in equation (13). Dust concentration at the midplane does not change the gas velocity profile significantly. The non-dimensional stopping time of the gas is $T_{s,g} = (\rho_g / \rho_d) T_s$. In order for the gas velocity profile to be affected by the dust, $T_{s,g}$ must be less than unity, i.e., $\rho_d / \rho_g > T_s$. At 50 AU, bodies of 1 m have $T_s \approx 20$, thus $T_{s,g} < 1$ requires that the dust layer's thickness is less than $f_{\text{dust}} T_s^{-1} \approx 5 \times 10^{-4}$ of the gas disk thickness. We assume that the turbulence of the gas disk is strong enough to prevent such a thin dust layer. The particle physical density is $\rho_p = 1 \text{ g cm}^{-3}$, assuming that bodies as large as 1 m are compacted.

Bodies of 1 m cannot survive for 10^6 years, as shown in Figure 8a. Dust grains have to grow up to at least 10 m in order to reside in the disk more than 10^6 yr. However, bodies larger than 10 m cannot emit millimeter continuum effectively. Figure 4 of Miyake & Nakagawa (1993) shows that if most of the dust mass is confined in 10 m bodies, the emissivity at a wavelength of 1 mm is three orders of magnitude less than the value for 1 mm grains.

In conclusion, the lifetime of dust disks is controlled by the dust migration time-scale, although a gas disk with a low viscosity ($\alpha \sim 10^{-3}$) can survive much longer than the dust disk. A dust disk composed of 1 mm compact ($\rho_p \approx 1 \text{ g cm}^{-3}$) grains in a low mass ($M_g \approx 2.5 \times 10^{-2} M$) gas disk cannot survive for 10^6 yr. We need $\rho_p \approx 0.1 \text{ g cm}^{-3}$ grains or a massive ($M_g \approx 2.5 \times 10^{-1} M$) gas disk in order to explain the

observed dust emission around CTTs of ages $\lesssim 1$ Myr. Survival of 1 cm grains is much harder than 1 mm grains.

5. Constraint on the Dust Growth Time

As shown in §4.2, dust grains of 1 cm hardly survive the rapid accretion for 10^6 yr, while observations suggest that grains around some CTTs as old as $10^6 - 10^7$ yr are larger than 1 mm. This implies one of the following possibilities: (1) A large enough amount of 1 mm grains needed to explain the observed millimeter flux is conserved for more than 10^6 yr without growing to 1 cm. Some part of the dust may have grown up to 1 cm and been removed from the disk. As the number density of 1 mm grains decreases, the growth time-scale becomes longer and the residual 1 mm grains keep their small sizes for more than 10^6 yr. (2) When grains grow beyond a critical size, at which $T_s = 1$, the radial velocity decreases as their sizes grow, as seen from equation (15). The dust grains around CTTs have already grown large enough (~ 10 m) to be decoupled from the gas and keep their orbits steady for 10^6 yr. The grains must grow quickly enough to avoid a large migration at the critical size. In addition, the optical depth of the disk must be large enough to explain the observed millimeter flux. Because only bodies larger than

10 m can reside in the disk for 10^6 yr and such large bodies cannot emit millimeter continuum effectively, millimeter sized grains must be produced from the larger bodies. (3) The rapid accretion of grains removes most of the dust from the disk in a time-scale less than 10^6 yr, but new dust is continuously replenished from the outside, such as an envelope that surrounds the disk.

If the possibilities (1) or (2) are the case, we can derive a constraint on the growth time-scale of the dust. In this section, we consider the dust growth time-scale using a simple analytical estimation.

5.1. Growth Time-scale

Dust grains collide with other grains and stick together to grow. We assume that growth of the largest grains occurs mainly through collisions among the largest grains, because the dust mass is dominated by them, as discussed in §2.4. We also assume that the grains well couple to the gas ($T_s < 1$). The growth of the largest grain is writ-

ten as

$$\frac{dm_d}{dt} = \frac{d}{dt} \frac{4}{3} s^3 \rho_p = C_{stk} (2s)^2 v_d v; \quad (25)$$

where the sticking parameter C_{stk} is the probability of coagulation per collision, ρ_d is the dust mass density at the midplane, and v is the relative velocity of collisions. The collisional cross section of equal-sized grains is $(2s)^2$. The sticking parameter is unknown and we discuss the constraint on it.

The collision velocity comes from the turbulent motion, the radial drift, and the sedimentation of grains. The relative velocity of two grains in the turbulent gas is $v_t \sim v_{turb} \sqrt{\frac{\rho_p}{\rho_g T_s}} \sim \sqrt{\frac{\rho_p}{\rho_g T_s}} c$ for grains of $T_s < 1$ (Volk et al. 1980), where we assume that the largest eddies have a typical velocity $v_{turb} \sim \sqrt{\frac{\rho_p}{\rho_g}}$ and a typical turnover time τ_K (Cuzzi et al. 2001). The relative velocity due to radial drift is $v_d \sim T_s v_K$ (see eq. [15]), and that due to sedimentation is $v_z \sim (z=r) T_s v_K$ (eq. [14] of Takeuchi & Lin 2003). For grains with small T_s , the turbulent motion controls the collision velocity, and $v \sim v_t$. In the equilibrium state of the vertical density distribution of the dust, the grain sedimentation is balanced by the turbulent diffusion. Hence, the relative velocity due to the sedimentation, v_z , is similar to or smaller than that from the turbulence and can be neglected ($v_z \sim (h_d=r) T_s v_K \sim \sqrt{\frac{\rho_p}{\rho_g T_s}} c \sim v_t$, where h_d is the scale height of the dust disk and eq. [29] below is used.) The condition for $v_t > v_d$ is

$$T_s < \frac{h_g^2}{2r^2} = \frac{h_g}{r} \ll 1; \quad (26)$$

where equation (20), $\rho_p = 10^{-3}$ and $(h_g=r) \ll 1$ is used. For grains of $T_s \sim 1$, the collision velocity is determined by the radial drift, and $v \sim v_d$.

The midplane dust density is estimated by

$$\rho_d = \frac{\rho_p}{2 h_d}; \quad (27)$$

where the same relation between the surface and midplane gas densities of equation (18) is applied to the dust. If dust grains are small enough to be well mixed to the gas, i.e., in the limit of small T_s , then $h_d = h_g$. For relatively large grains, the dust sediments to the midplane and the thickness of the dust disk is smaller than that of the gas. As derived in equation (34) in Paper I (with the Schmidt

number $Sc = 1$), the dust disk scale height becomes

$$h_d = 2 \ln \frac{1}{T_s} + 1 \sqrt{\frac{\rho_p}{\rho_g}} h_g \sim \frac{2}{T_s} \sqrt{\frac{\rho_p}{\rho_g}} h_g; \quad (28)$$

for $T_s \ll 1$. Because h_d cannot be larger than h_g , the approximated scale height is expressed as

$$h_d = \min \left(1; \frac{2}{T_s} \sqrt{\frac{\rho_p}{\rho_g}} h_g \right); \quad (29)$$

which is applicable for $T_s < 1$.

The growth time-scale is defined as an e-folding time in size. From equations (25), (27), and (29), it becomes

$$\tau_{grow} = \frac{s}{ds/dt} = \frac{\rho_p}{C_{stk} \rho_d} \sqrt{\frac{\rho_g}{\rho_p}} \min \left(1; \frac{2}{T_s} \sqrt{\frac{\rho_p}{\rho_g}} h_g \right); \quad (30)$$

For grains that have $2 < T_s < (r=h_g)^2$, the growth time-scale reduces to

$$\tau_{grow} = \frac{4}{C_{stk}} \frac{g}{\rho_d} \tau_K^{-1}; \quad (31)$$

where $v \sim v_t \sim \sqrt{\frac{\rho_p}{\rho_g T_s}} c$ and equations (8) and (21) are used. In this range of T_s , the growth time is independent of the grain size s .

5.2. Slow Growth

We first consider the possibility that grains keep their sizes less than 1 cm to avoid rapid accretion for more than 10^6 yr.

Grains of 1 cm with $\rho_p = 0.1 \text{ g cm}^{-3}$ satisfy the condition $2 < T_s < (r=h_g)^2$ if they are in 5 AU $\leq r \leq 200$ AU of a disk with $\rho_g = 10^{-3}$ and $(h_g=r) \ll 1$ (see the $A = 1$ line in Fig. 2). For such grains, the growth time-scale is calculated by equation (31). Inside 5 AU, it is calculated by equation (30) with $v \sim v_d$. Figure 9 shows the growth time-scale for various values of the sticking parameter C_{stk} . If grains stick effectively ($C_{stk} \sim 0.1$), the growth time is less than 10^6 yr in most part of the disk ($r \leq 200$ AU). It is thus expected that grains rapidly grow up to 1 cm and are quickly removed. If the sticking parameter is $C_{stk} = 10^{-2}$, dust growth in the outer disk ($r \gtrsim 40$ AU) takes more than 10^6 yr and the outer dust disk can survive.

In order to see the effect of dust growth, we put a sink term ,

$$-\dot{\sigma}_d = \frac{\dot{\sigma}_d}{\tau_{\text{grow}}} ; \quad (32)$$

in the right hand side of equation (13). In this treatment, we assume that on a time-scale τ_{grow} the dust grains grow from 1 mm to 1 cm and are removed from the disk. The growth time-scale τ_{grow} is the e-folding time in the size, and the actual growth time from 1 mm to 1 cm is probably longer by a factor, $\ln 10 \approx 2.3$, but we neglect the difference of this factor.

Figure 10 shows the density evolution of the dust with the sticking parameter $C_{\text{stk}} = 10^{-1}$. The grains first grow quickly with a much shorter time-scale than the migration time-scale. As the dust density decreases, the growth time-scale increases (see eq. [31]) and finally becomes as large as the age of the disk. (The dust growth itself cannot enlarge the growth time beyond the age of the disk.) In 10^5 yr, the growth time-scale has become similar to the age (10^5 yr) in the entire dust disk. At this stage, the growth time is almost constant with r . From equation (31), a constant growth time means that the surface density profile of the dust approaches $\sigma_d / \sigma_g = \kappa / r^{1/2}$. At $t = 10^6$ yr, the growth time increases to 10^6 yr, which is comparable to the dust migration time-scale. After that, grain migration affects the shape of the density profile. Figure 11 shows the time evolution of the dust thermal emission for various values of the sticking parameter C_{stk} . If dust growth is effective and $C_{\text{stk}} \approx 1$, the dust disk cannot survive for 10^6 yr and the thermal emission quickly decays. To explain the observed dust emission, the sticking parameter must be less than 0.1 .

The slow growth scenario may cause a difficulty in forming planets at large distances from the star (> 40 AU). We assumed that grains in the outer part of the disk keep their sizes smaller than 1 cm for 10^6 yr. After 10^6 yr, the grains have grown to 1 cm, however, and they start rapid accretion and disappear or at least migrate to the inner part of the disk before growing to planetesimals. In this scenario, it is difficult to form planets in the outer region of the disk, though planet formation may be possible in the inner disk.

5.3. Fast Growth

The other possibility is that the dust grains have already grown large enough to stop their migration. After the grain size becomes larger than the critical size, at which T_s is unity, the grains' radial motion slows down as they grow larger (see eq. [15] and Fig. 1). Finally, the grains completely decouple from the gas and stop in the disk. Before they grow up to such large bodies, however, they must survive the period of rapid migration.

When $T_s = 1$, the radial velocity reaches the maximum value, $v_{d,\text{max}} = (\approx 2) v_K$, and the migration time τ_{dust} becomes minimum ,

$$\tau_{\text{dust,min}} = \frac{r}{v_{d,\text{max}}} = 2^{-1} \frac{1}{\kappa} : \quad (33)$$

(The dust disk thickness of $T_s = 1$ grains is $\frac{1}{2} h_g$ as seen in eq. [28]. The midplane dust density is increased by a factor $(2)^{-1/2}$, but as long as $\sigma_d > 10^{-4}$, the dust density does not exceed the gas density and the gas velocity profile is not modified.) From expression (21) of the non-dimensional stopping time in Epstein's gas drag law, the grain size at $T_s = 1$ is

$$s = \frac{2}{\kappa} \frac{g}{\rho} : \quad (34)$$

(Epstein's law is valid for grains smaller than 10 μm at 10 AU and smaller than 10 km at 100 AU.) In order to survive rapid migration, the dust must grow quickly and pass through this hazardous period before falling into the star. The growth time-scale is, from equations (30) and (34) with $v' = v_{d,\text{max}}$ and $T_s = 1$,

$$\tau_{\text{grow}} = \frac{4^p - 1}{C_{\text{stk}}} \frac{g h_g}{v_{d,\text{max}}} : \quad (35)$$

The condition $\tau_{\text{grow}} < \tau_{\text{dust,min}}$ becomes

$$\frac{\dot{\sigma}_d}{\sigma_g} > \frac{4^p - 1}{C_{\text{stk}}} \frac{h_g}{r} : \quad (36)$$

Hence, the dust-to-gas ratio must be larger than certain values, and this condition is independent of the dust properties. Figure 12 shows the values of the right hand side of equation (36) for $C_{\text{stk}} = 0.1$ and 1 (and $\kappa = 10^{-3}$). The condition $\tau_{\text{grow}} < \tau_{\text{dust,min}}$ is satisfied if the value of $\dot{\sigma}_d / \sigma_g$ is above the solid lines. If we assume the

dust-to-gas ratio is $f_{\text{dust}} = \rho_{\text{d}}/\rho_{\text{g}} = 10^{-2}$, the sticking parameter C_{stk} must be close to unity in order for the dust to grow fast enough (at $r \sim 300$ AU). If the grains are as less sticky as $C_{\text{stk}} = 0.1$, the migration dominates the growth.

After the grains pass the fast migration period, they still continue to grow. In order that grains may reside in the disk for 10^6 yr, their sizes must be larger than $10 \mu\text{m}$, as shown in x4.4. However, observed millimeter continuum is probably not emitted from such large bodies. Thus, grains of 1 mm need to be continuously replenished through collisions of the large bodies, or from an envelope covering the disk.

One possibility of accounting for the grain growth and the millimeter flux at the same time is assuming a high value of the dust-to-gas ratio. It is possible to keep the millimeter flux as high as the observed values of some CTTSs for 10^6 yr, if the sticking probability is $C_{\text{stk}} = 0.1$ (see Fig. 11). It is also possible for grains inside 20 AU to survive the rapid accretion phase, if the dust-to-gas ratio is as large as 0.05, for the same sticking probability $C_{\text{stk}} = 0.1$ (see Fig. 12). Hence, if the dust-to-gas ratio is several times higher than the solar abundance and if the sticking probability is of order of 0.1, then grains of millimeter size in the outer part of the disk can continue to emit sufficient millimeter continuum, and grains in the inner disk (< 20 AU) can grow fast enough to survive the rapid accretion phase. Calculations including both grain growth and radial migration are needed to examine this possibility.

6. Summary

Motivated by radio observations suggesting grain growth to 1 mm or larger in CTTS disks, we studied the evolution of dust disks whose main components are millimeter sized grains.

1. Gas drag on millimeter sized grains accelerates the dust disk accretion to the star. When grains grow to 1 cm , they cannot reside in the disk for over 10^6 yr, and as the dust disk accretes, its millimeter continuum emission decreases. The lifetimes of grains are longer for a smaller particle physical density (i.e., ρ_{p}), and in a more massive gas disk.

2. If the observed millimeter continuum of CTTSs comes from millimeter sized grains, a suf-

ficient amount of grains in this size range must exist more than 10^6 yr in their disks. This suggests one of the following possibilities. One is that millimeter sized grains do not grow rapidly, and it takes more than 10^6 yr to become larger than 1 cm . If the grains' sticking probability is less than

0.1, this condition is satisfied in the outermost region of the disk ($r \gtrsim 100$ AU). Another possibility is that the grains have already grown to $10 \mu\text{m}$ or larger and they do not migrate rapidly anymore, and millimeter sized grains are continuously replenished through collisions of the large bodies. If the disk's dust-to-gas ratio is > 0.1 and the sticking probability is $C_{\text{stk}} > 0.1$, the observable millimeter continuum holds for more than 10^6 yr, emitted mainly from grains of 1 mm in the outer disk, and in the inner disk the grains can grow larger than $10 \mu\text{m}$ before falling to the star. The other possibilities are that millimeter sized grains are replenished from a surrounding envelope, or that the small end of the observed millimeter continuum is not due to dust growth. In order to examine these possibilities, we need to perform simulations taking account of both dust migration and dust growth at the same time.

We gratefully acknowledge useful discussions with Cathie Clarke, which drew our attention to this problem. We are also grateful to Sozo Yokogawa and Yoichi Itoh for useful comments, and to Anthony Toigo for careful reading of the manuscript. We acknowledge helpful comments from the referee. This work was supported in part by an NSF grant AST 99 87417 and in part by a special NASA astrophysical theory program that supports a Joint Center for Star Formation Studies at UC Berkeley, NASA-Ames Research Center, and UC Santa Cruz. This work was also supported by NASA NAG 5-10612 through its Origin program, JPL 1228184 through its SIM program, and the 21st Century COE Program of MEXT of Japan, "the Origin and Evolution of Planetary Systems."

REFERENCES

- Adachi, I., Hayashi, C., & Nakazawa, K. 1976, Prog. Theor. Phys. 56, 1756
- Adams, F. C., Lada, C. J., & Shu, F. H. 1988, ApJ, 326, 865

- Arm itage, P. J., Clarke, C. J., & Palla, F. 2003, *MNRAS*, 342, 1139
- Bath, G. T., & Pringle, J. E. 1981, *MNRAS*, 194, 967
- Beckwith, S. V. W., Henning, T., & Nakagawa, Y. 2000, in *Protostars and Planets IV*, eds. Mannings, V., Boss, A. P., & Russell, S. S. (Tucson: University of Arizona Press), 533
- Beckwith, S. V. W., & Sargent, A. I. 1991, *ApJ*, 381, 250
- Beckwith, S. V. W., Sargent, A. I., Chini, R. S., & Gusten, R. 1990, *AJ*, 99, 924
- Cuzzi, J. N., Hogan, R. C., Paque, J. M., & Dobrovolskis, A. R. 2001, *ApJ*, 546, 496
- Dutrey, A., Guilloteau, S., Duvert, G., Prato, L., Simon, M., Schuster, K., & Menard, F. 1996, *A & A*, 309, 493
- Duvert, G., Guilloteau, S., Menard, F., Simon, M., & Dutrey, A. 2000, *A & A*, 355, 165
- Hartmann, L., Calvet, N., Gullbring, E., & D'Alessio, P. 1998, *ApJ*, 495, 385
- Hayashi, C., Nakazawa, K., & Nakagawa, Y. 1985, in *Protostars and Planets II*, ed. D. C. Black & M. S. Matthews (Tucson: Univ. of Arizona Press), 1100
- Hellyer, B. 1970, *MNRAS*, 148, 383
- Hogerheijde, M. R., Johnstone, D., Matsumura, I., Jayawardhana, R., & Muzerolle, J. 2003, *ApJ*, 593, L101
- Kenyon, S. J., & Hartmann, L. 1995, *ApJS*, 101, 117
- Kitamura, Y., Momose, M., Yokogawa, S., Kawabe, R., Tamura, M., & Ida, S. 2002, *ApJ*, 581, 357
- Lin, D. N. C., & Papalizou, J. C. B. 1986, *ApJ*, 309, 846
- Lynden-Bell, D., & Pringle, J. E. 1974, *MNRAS*, 168, 603
- Mannings, V., & Emerson, J. P. 1994, *MNRAS*, 267, 361
- Mather, J. S., Ruppel, W., & Nordsieck, K. H. 1977, *ApJ*, 217, 425
- Miyake, K., & Nakagawa, Y. 1993, *Icarus*, 106, 20
- Mizuno, H., Markiewicz, W. J., & Volk, H. J. 1988, *A & A*, 195, 183
- Nakagawa, Y., Sekiya, M., & Hayashi, C. 1986, *Icarus*, 67, 375
- Ohashi, N., Kawabe, R., Ishiguro, M., & Hayashi, M. 1991, *AJ*, 102, 2054
- Ohashi, N., Hayashi, M., Kawabe, R., & Ishiguro, M. 1996, *ApJ*, 466, 317
- Osterloh, M., & Beckwith, S. V. W. 1995, *ApJ*, 439, 288
- Press, W. H., Flannery, B. P., Teukolsky, S. A., & Vetterling, W. T. 1992, *Numerical Recipes in Fortran* (Cambridge University Press)
- Schneider, G., et al. 1999, *ApJ*, 513, L127
- Shakura, N. I., & Sunyaev, R. A. 1973, *A & A*, 24, 337
- Takeuchi, T., & Lin, D. N. C. 2002, *ApJ*, 581, 1344, (Paper I)
- Takeuchi, T., & Lin, D. N. C. 2003, *ApJ*, 593, 524
- van de Hulst, H. C. 1981, *Light Scattering by Small Particles* (New York: Dover)
- van Leer, B. 1977, *J. Comput. Phys.*, 23, 276
- Volk, H. J., Morill, G. E., Roeder, S., & Jones, F. C. 1980, *A & A*, 85, 316
- Weidenschilling, S. J. 1977, *MNRAS*, 180, 57
- Yoshida, F., Nakamura, T., Watanabe, J., Kinoshita, D., Yamamoto, N., & Fuse, T. 2003, *PASJ*, 55, 701

This 2-column preprint was prepared with the AAS L^AT_EX macros v5.0.

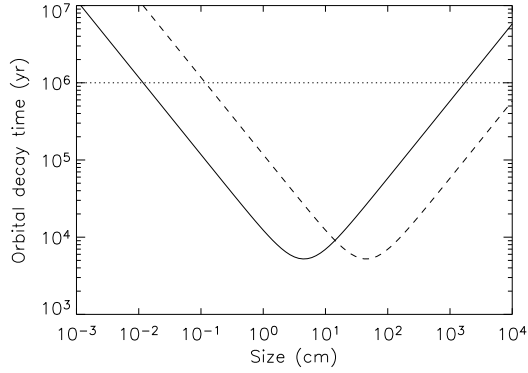


Fig. 1. | Orbital decay time, t_{dust} , of dust grains at 50 AU in a gas disk. The solid line represents the orbital decay time of compact grains of physical density $\rho_p = 1 \text{ g cm}^{-3}$, and the dashed line shows that of fluffy grains of $\rho_p = 0.1 \text{ g cm}^{-3}$. The decay time is calculated at the midplane of the model disk described in §3.1, but ignoring the gas accretion velocity ($v_g = 0$). The dotted line represents a reference time scale of 10^6 yr .

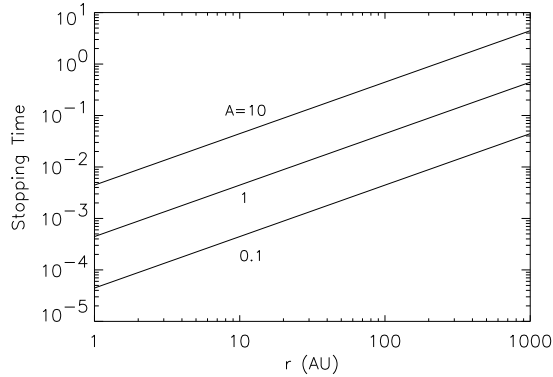


Fig. 2. | Non-dimensional stopping time of a dust grain for various models. From the upper line, $A = 10, 1$, and 0.1 , respectively. Model $A = 1$ is the fiducial model, which have for example $M_g = 2.5 \times 10^2 M_\oplus$, $\rho_p = 1 \text{ g cm}^{-3}$, and $s = 1 \text{ mm}$. Model $A = 0.1$ represents for example a lower physical density of a grain ($\rho_p = 0.1 \text{ g cm}^{-3}$) or a higher gas disk mass ($M_g = 0.25 M_\oplus$). Model $A = 10$ represents for example a larger grain size ($s = 1 \text{ cm}$). In this figure, the power-law gas density profile is extrapolated to 1000 AU. The gas mass M_g represents the mass within 100 AU.

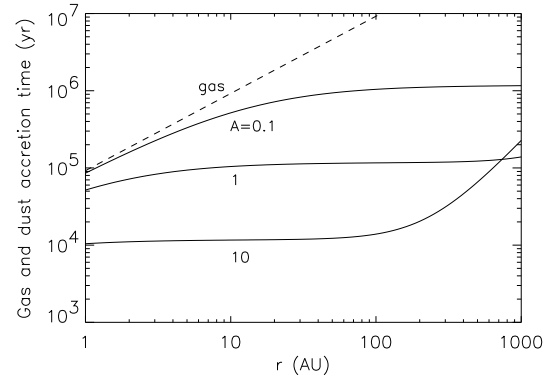


Fig. 3. | Accretion time-scales of the gas and the dust in the fiducial model defined in §3.1. The dashed line shows the gas accretion time-scale, t_{gas} , calculated for $\dot{M} = 10^{-3}$. The solid lines show the dust migration time-scales, t_{dust} , of the models for $A = 0.1, 1$, and 10 , respectively, from the upper line. In all models, the gas accretion time t_{gas} is the same. The power-law gas density profile is extrapolated to 1000 AU.

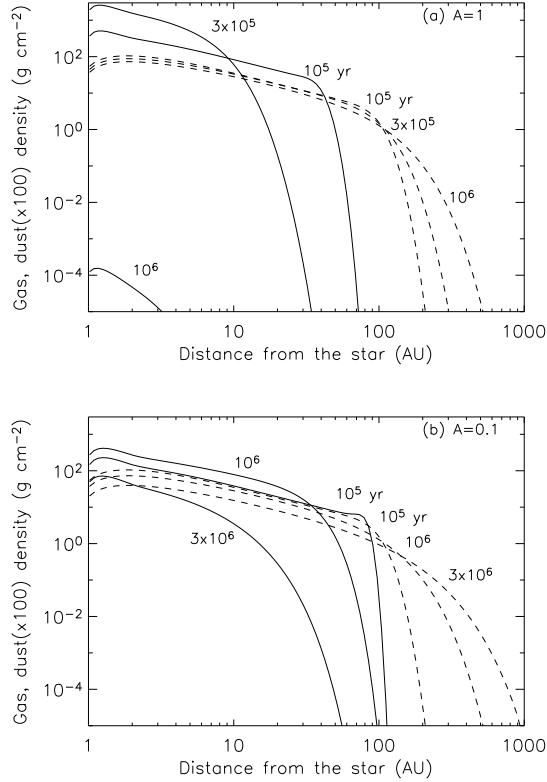


Fig. 4. Evolution of the gas and dust surface densities of a low viscous disk ($\alpha = 10^{-3}$). The values of the dust surface densities are multiplied by $f_{\text{dust}}^1 = 100$ and shown by the solid lines. The dashed lines show the gas surface densities. (a) $A = 1$, i.e., for example, $M_g = 2.5 \times 10^2 M_\oplus$, $\rho_p = 1 \text{ g cm}^{-3}$, and $s = 1 \text{ mm}$. (b) $A = 0.1$, i.e., for example, $\rho_p = 0.1 \text{ g cm}^{-3}$ or $M_g = 0.25 M_\oplus$. (In the $M_g = 0.25 M_\oplus$ case, the labels of the y-axis must be read as 10 times larger values.)

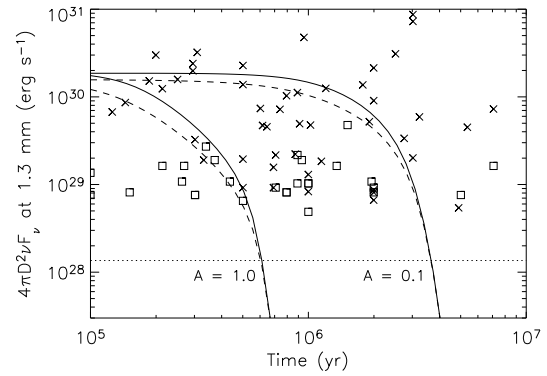


Fig. 5. Evolution of the dust thermal emission at a wavelength of 1.3 mm for a low viscous disk ($\alpha = 10^{-3}$) viewed face-on ($i = 0^\circ$). The solid lines are for models of $A = 1$ and 0.1 , respectively, from the left. The initial disk mass is $M_g = 2.5 \times 10^2 M_\oplus$. The dashed lines show the fluxes of inclined ($i = 60^\circ$) disks for comparison. Crosses are the observed values of T Tauri stars taken from Beckwith et al. (1990) and Osterloh & Beckwith (1995). Squares show the upper limits of 1.3 mm fluxes. The dotted line is the detection limit, 2.5 mJy, of the observation by Duvert et al. (2000). The distance $D = 140 \text{ pc}$ is assumed.

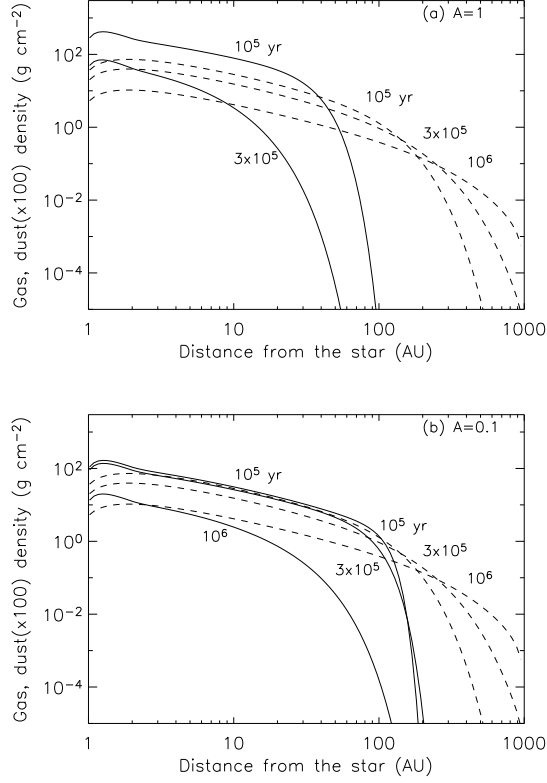


Fig. 6. Same as Fig. 4, but for a high viscosity disk ($\nu = 10^2$). (a) $A = 1$. At 10^6 yr, the dust surface density is below the y-range of the figure. (b) $A = 0.1$.

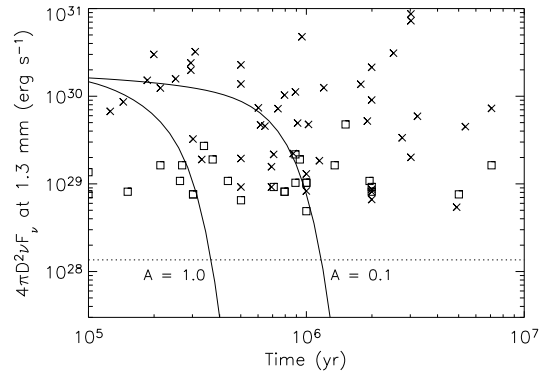


Fig. 7. Same as Fig. 5, but for a high viscosity disk ($\nu = 10^2$).

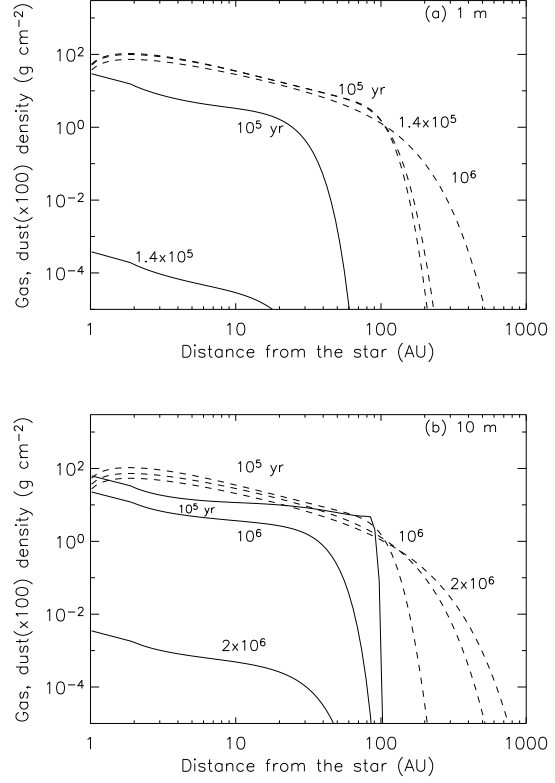


Fig. 8. Same as Fig. 4, but for large bodies. (a) $s = 1$ m, $p = 1$ g cm $^{-3}$. (b) $s = 10$ m.

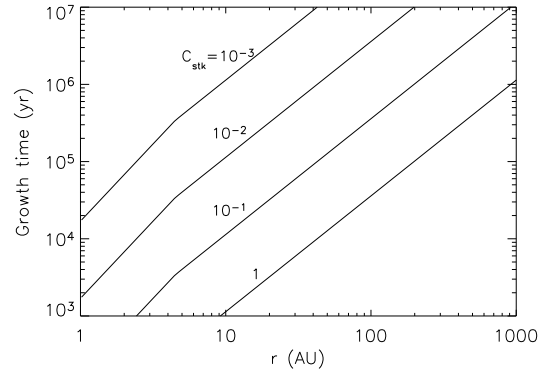


Fig. 9. Dust growth time-scale, t_{grow} , for various sticking parameters C_{stk} . The disk is at the initial state ($t = 0$) of the dust model described in §3.1.

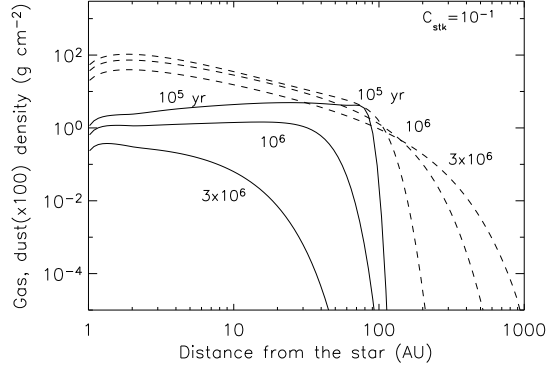


Fig. 10. Same as Fig. 4, but with dust removal through its growth. The sticking probability is $C_{\text{stk}} = 0.1$. The dust parameters are $s = 1 \text{ mm}$, $\rho = 0.1 \text{ g cm}^{-3}$.

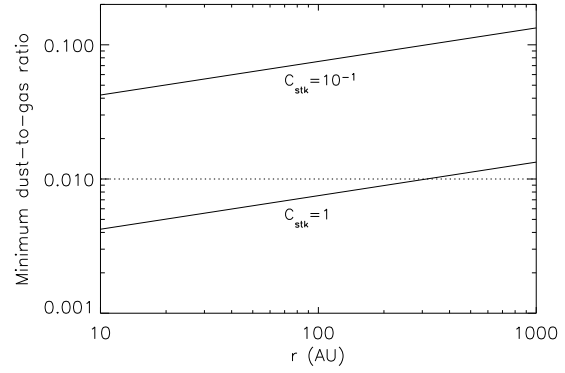


Fig. 12. Condition on the dust-to-gas ratio for dust survival by fast growth, given by equation (36). The disk is in the initial state ($t = 0$) of the dust model described in §3.1. The condition, $\rho_{\text{grow}} < \rho_{\text{dust, min}}$, is satisfied above the upper solid line for $C_{\text{stk}} = 0.1$ and above the lower solid line for $C_{\text{stk}} = 1$. The dotted line shows the dust-to-gas ratio $f_{\text{dust}} = 10^{-2}$. The figure shows only $r > 10 \text{ AU}$, where Epstein's gas drag law is valid.

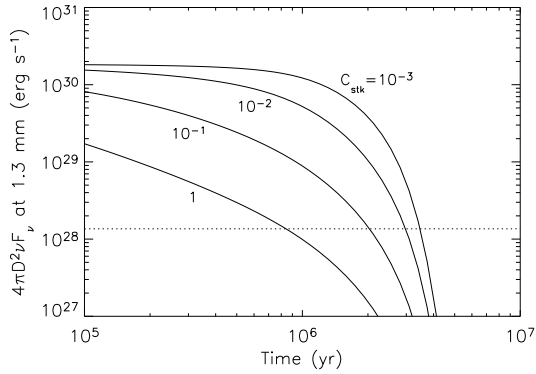


Fig. 11. Same as Fig. 5, but with dust removal through its growth. The sticking parameters are $C_{\text{stk}} = 10^{-3}, 10^{-2}, 10^{-1}$, and 1, respectively, from the upper line.